Diabetologia (2013) 56:533–541
DOI 10.1007/s00125-012-2806-8

ARTICLE

Hydrogen sulfide-induced inhibition of L-type Ca^{2+} channels and insulin secretion in mouse pancreatic beta cells

G. Tang · L. Zhang · G. Yang · L. Wu · R. Wang

Received: 29 June 2012 / Accepted: 29 November 2012 / Published online: 30 December 2012

Abstract
Aims/hypothesis L-type voltage-dependent Ca^{2+} channels (VDCCs) in pancreatic beta cells play a critical role in regulating insulin secretion. The gasotransmitter H_2S is mostly generated from L-cysteine in pancreatic beta cells by cystathionine γ-lyase (CSE) and has been reported to inhibit insulin release by opening ATP-sensitive K^+ channels. However, whether and how H_2S affects VDCCs in beta cells is unknown.
Methods The whole-cell patch-clamp technique was used to record VDCCs in beta cells from *Cse* (also known as C*th*)-knockout (KO) and wild-type (WT) mice. Insulin secretion from pancreatic islets and endogenous H_2S production in pancreas were measured.
Results The H_2S donor NaHS reversibly decreased L-type VDCC current density in a concentration-dependent fashion in WT pancreatic beta cells, and the current density was further inhibited by nifedipine. Furthermore, NaHS inhibited the channel recovery from depolarisation-induced inactivation, but did not shift the current–voltage (*I–V*) relationship. ACS67, another H_2S donor, also inhibited L-type VDCCs in beta cells. Inhibiting CSE activity with DL-propargylglycine increased the basal L-channel activity of beta cells from WT mice, but not that of beta cells from *Cse*-KO mice. Beta cells from *Cse*-KO mice displayed higher L-type VDCC density than those from WT mice. Insulin secretion from pancreatic islets was elevated in *Cse*-KO mice compared with WT mice. NaHS dose-dependently inhibited glucose-stimulated insulin secretion, which was further inhibited by nifedipine. Bay K-8644 increased glucose-stimulated insulin secretion, but this was counteracted by NaHS and nifedipine.
Conclusions/interpretation Exogenous and endogenous H_2S inhibit L-type VDCC activity and pancreatic insulin secretion, constituting a novel mechanism for the regulation of insulin secretion by the CSE/H_2S system.

Keywords Beta cells · Ca^{2+} channels · H_2S · Insulin secretion · Pancreas

Abbreviations

$[Ca^{2+}]_i$	Intracellular calcium concentration
CBS	Cystathionine β-synthase
CSE	Cystathionine γ-lyase
HP	Holding potential
I_{Ca}	VDCC current
$I_{Ca,peak}$	Peak I_{Ca}
$I_{Ca,SS}$	Steady-state I_{Ca}
I–V	Current–voltage
K_{ATP}	ATP-sensitive K^+
KO	Knockout
KRB	Krebs–Ringer bicarbonate
PPG	DL-propargylglycine
STZ	Streptozotocin
VDCC	Voltage-dependent Ca^{2+} channel
WT	Wild-type
ZDF	Zucker diabetic fatty

G. Tang · L. Zhang · R. Wang (✉)
Department of Biology, Lakehead University, 955 Oliver Road, Thunder Bay, ON P7B 5E1, Canada
e-mail: rwang@lakeheadu.ca

G. Yang
School of Kinesiology, Lakehead University, Thunder Bay, ON, Canada

L. Wu
Department of Health Sciences, Lakehead University, Thunder Bay, ON, Canada

L. Wu
Thunder Bay Regional Research Institute, Thunder Bay, ON, Canada

Introduction

Cystathionine γ-lyase (CSE) uses L-cysteine as a substrate to generate H_2S in many types of mammalian cells [1, 2]. CSE is mostly responsible for the endogenous production of H_2S in pancreatic tissues and cloned pancreatic beta cell lines [2–8]. The inhibition of CSE activity by DL-propargylglycine (PPG) significantly decreased production of H_2S and increased plasma insulin levels in Zucker diabetic fatty (ZDF) rats [6], while increased *Cse* expression and H_2S formation were observed in streptozotocin (STZ)-induced diabetic rats [4, 6, 8]. Genetic deletion of *Cse* (also known as *Cth*) in mice markedly reduces H_2S levels in different tissues, leading to increased blood pressure, accumulation of homocysteine and impairment of vascular endothelial functions [3]. When stimulated with high glucose (20 mmol/l), insulin secretion from pancreases of *Cse*-knockout (KO) mice is significantly increased [4]. Compared with wild-type (WT) mice, *Cse*-KO mice that receive STZ injections have a delayed onset of diabetic status [4]. STZ significantly increases pancreatic H_2S production in WT mice, but not in *Cse*-KO mice, and it causes more apoptotic beta cell death in WT than in *Cse*-KO mice.

Voltage-dependent Ca^{2+} channels (VDCCs) in pancreatic beta cells play a critical role in the regulation of insulin secretion via controlling Ca^{2+} influx. It has been reported that H_2S stimulates ATP-sensitive K^+ (K_{ATP}) channels, which hyperpolarises cell membrane and indirectly inactivates L-type VDCCs, leading to reduced insulin secretion [5, 9–11]. Interaction between H_2S and K_{ATP} channels in insulin-secreting cells constitutes an important regulatory mechanism for insulin secretion [10, 11]. On the other hand, the role of L-type VDCCs in H_2S-regulated insulin secretion is unknown. One report described an inhibitory effect of H_2S on L-type VDCCs in isolated rat cardiomyocytes [12]. Another study in cerebellar granule neurons reported the contradictory result that H_2S increased intracellular Ca^{2+} concentration ($[Ca^{2+}]_i$) by stimulating L-type VDCCs [13]. Whether and how H_2S interacts with L-type VDCCs in beta cells is intriguing and warrants in-depth investigation.

In the present study, *Cse*-KO and WT mice were used to isolate pancreatic beta cells. The effects of NaHS, a donor of H_2S, were first determined on the electrophysiological properties of L-type VDCCs. Changes in L-type VDCCs were also tested in the presence of a CSE inhibitor (PPG) or in the absence of endogenous H_2S. The insulin secretion from and H_2S production in islets or pancreas were measured with or without blocking L-type VDCCs.

Methods

Animal preparation The *Cse*-KO mice were generated and house bred as previously described [3]. The fourth generation of 10- to 16-week-old male *Cse*-KO offspring and age-matched male WT littermates on a C57BL/6 J×129SvEv background were used. All animal experiments were approved by the Animal Use Committee of Lakehead University, ON, Canada.

Isolation of intact islets and beta cells from mouse pancreas Briefly, the mice were anaesthetised with a single intraperitoneal injection of ketamine (2.2 mg/10 g body weight) and xylazine (0.44 mg/10 g body weight) before the opening of the abdominal wall. The pancreas was distended by injection of 1 ml Krebs–Ringer bicarbonate (KRB) containing 0.5–1 mg/ml collagenase type V (Sigma, USA), 0.5–1 μl/ml DNase I (Sigma, USA) and bovine serum albumin (0.5 mg/ml) through a cannula inserted into the common bile duct. KRB comprised: NaCl 129 mmol/l; KCl 4.8 mmol/l; KH_2PO_4 1.2 mmol/l; $NaHCO_3$ 5 mmol/l; $MgCl_2$ 1.2 mmol/l; HEPES 10 mmol/l; and $CaCl_2$ 2.5 mmol/l. The pancreas was then removed carefully and transferred to a 50 ml Falcon tube with the above enzyme solution, and incubated for 5–10 min in a water bath at 37°C. Cleaned islets of Langerhans were hand-picked under a dissecting microscope after ×3 centrifuge washout (at 1,500 *g* for 3 min at 4°C) with Ca^{2+}/Mg^{2+}-free KRB. The dispersed islets were dissociated into single cells by vigorous shaking in Ca^{2+}/Mg^{2+}-free KRB supplemented with ×1 enzyme-free cell-dissociation reagent (HiMedia Lab Pvt. Ltd, VWR, Mississauga, ON, Canada). The dispersed islet cells were cultured on small glass cover slips pre-coated with poly L-lysine, in RPMI 1640 medium supplemented with 10% (vol./vol.) fetal bovine serum, 100 U/ml penicillin, and 10 μg/ml streptomycin in humidified air at 37°C containing 5% CO_2. Primary-cultured (1–3 days) islet cells were used in the patch-clamp experiments.

Measurement of insulin secretion from isolated pancreatic islets Freshly isolated islets (ten size-matched for each batch) were washed and pre-incubated with glucose-free RPMI 1640 medium in 24 well plates [6]. After pre-incubation for 30 min, islets were treated for 30 min at 37°C with different chemicals in the presence of either 2.8 or 20 mmol/l glucose. In other experiments, insulin release from isolated islets was detected in KRB. At the end of each incubation period, the medium was collected and centrifuged for 10 min at 239 *g* to remove islet debris. The insulin level in the supernatant fraction was determined using the mouse insulin ELISA kit (Mercodia AB, Sylveniusgatan, Uppsala, Sweden). After insulin measurement, the islets were scraped from 24 well plates on ice into the centrifuge tube; protein concentration was then measured using Bradford Reagent (Sigma, St Louis, MO, USA).

Electrophysiological recordings The patch-clamp technique was used to record whole-cell VDCC currents in the voltage-clamp mode [14, 15]. The glass cover slip with primary-

cultured pancreatic beta cells attached was inserted into the perfusion chamber, which was mounted on the stage of an inverted phase-contrast microscope (Olympus IX71, Olympus, Tokyo, Japan). Cells were washed with bath solution in the chamber for 3–5 min before starting an experiment. Patch pipettes were pulled from borosilicate glass capillaries with filaments (Sutter Instrument, Novato, CA, USA) with tip resistance of 2–5 MΩ when filled with different pipette solutions. Currents were recorded with an Axopatch 200-B amplifier (Axon Instruments, Molecular Devices, LLC, Sunnyvale, CA, USA), controlled by a Digidata 1200 interface and a pCLAMP software (Version 6.02, Axon Instruments). Membrane currents were filtered at 1 kHz with a four-pole Bessel filter. At the beginning of each experiment, the patch-clamp amplifier was adjusted to set I=0. No leakage subtraction was performed for the original recordings, and all cells with visible changes in leakage currents during the course of study were excluded from further analysis. The VDCC currents were recorded by a 300 ms step pulse ranging from −80 to +60 mV with 10 mV increments. The holding potentials (HPs) were set at −80 or −40 mV, at which the outward voltage-dependent K^+ currents or inward T-type VDCC currents were largely inactivated, respectively. The pipette solution for recording VDCC currents contained: Cs_2-aspartate 70 mmol/l, EGTA 10 mmol/l, MgATP 4 mmol/l, $MgCl_2$ 5 mmol/l, $CaCl_2$ 1 mmol/l, Na-pyruvate 5 mmol/l, K-succinate 5 mmol/l, glucose 25 mmol/l, HEPES 10 mmol/l, Na-creatine phosphate 5 mmol/l, creatine kinase 50 U/ml, Na_2GTP 0.3 mmol/l (pH=7.2). The bath solution for recording VDCC currents included: Trizma-HCl 110 mmol/l, TEA-Cl 5 mmol/l, $BaCl_2$ 20 mmol/l, CsCl 5 mmol/l, HEPES 20 mmol/l, glucose 5 mmol/l (pH=7.4). Giga-ohm seal was made in normal extracellular high-Na^+ solution: NaCl 135 mmol/l, KCl 4.8 mmol/l, $MgCl_2$ 1.2 mmol/l, $CaCl_2$ 2.5 mmol/l, HEPES 10 mmol/l. In some experiments, tetrodotoxin (TTX) at 1 μmol/l was included in the bath solution to block any Na^+ channel currents. The osmolality of recording solutions was adjusted to 290 mOsmol/l, and pH to 7.2–7.4. Cells were continuously superfused with the bath solution containing the test chemicals at the desired final concentrations. All experiments were performed at room temperature. In electrophysiological recordings, beta cells were distinguished from other islet cells by large size (usually capacitance ≥7 pF), no detectable Na^+ current when holding at −70 mV, and characteristic oscillatory or bursting electrical activity when exposed to 10 mmol/l glucose [16, 17].

The current density of L-type VDCCs was calculated by normalising the peak amplitude of current with cell capacitance (pA/pF). The channel recovery from depolarisation-induced inactivation was also produced by a double-pulse protocol stepped to 0 mV from −70 mV with an HP of −80 mV. An increase in the interval between the conditioning and test pulses resulted in a recovery of VDCC current (I_{Ca}), which can be fitted by a mono-exponential equation: $I/I_{max} = 1 - \exp(-t/\tau)$, where I_{max} is the current measured during the first pulse, I is the current measured during the second pulse, t represents the value of the interval, and τ represents the time constant of I_{Ca} recovery from inactivation.

Chemicals and statistical analysis Nifedipine, Bay K-8644, PPG, and NaHS were purchased from Sigma Chemicals, glibenclamide from Research Biochemicals International (Natick, MA, USA), and ACS 67 from Cayman Chemical Company (Ann Arbor, Michigan, USA). Stock solutions of nifedipine, glibenclamide and ACS 67 were made in DMSO and diluted to the desired concentrations immediately prior to use. DMSO alone was without effect at the concentration used (up to 0.3%, vol./vol.).

Data are expressed as means±SEM and were analysed using paired Student's t test and analysis of variance in conjunction with the Newman–Keuls test where applicable. Differences were considered statistically significant at the level of $p<0.05$.

Results

Electrophysiological features and pharmacological sensitivity of VDCC currents To separate the whole-cell I_{Ca} components—peak I_{Ca} ($I_{Ca,peak}$) with fast inactivation and a steady-state I_{Ca} current ($I_{Ca,SS}$) without inactivation—different HPs were employed. At the HP of –80 mV, I_{Ca} current traces were recorded by a 300 ms pulse stepped from −80 to +60 mV with 10 mV increments, exhibiting both $I_{Ca,peak}$ and $I_{Ca,SS}$ components (Fig. 1a). Changing the HP from −80 to −40 mV would inactivate T-type VDCCs [18, 19]. In our study, this HP change reduced the $I_{Ca,peak}$ density from −52.2±5.5 to −36.7±3.7 pA/pF (at +10 mV, n=8, $p<0.05$) (Fig. 1a,b). With the HP at −40 mV, the whole-cell inward I_{Ca} showed only one $I_{Ca,SS}$ component (Fig. 1a–c). This $I_{Ca,SS}$ had the same current density with −80 or −40 mV as the HPs (n=8, $p>0.05$) (Fig. 1c). To confirm whether $I_{Ca,SS}$ represents mostly the activity of L-type VDCCs, a specific agonist and an antagonist for L-type VDCC were applied. Bay K-8644, an agonist of L-type VDCC, enhanced the $I_{Ca,SS}$ by 53.3±4.2% and 53.8±6.4% (at +20 mV, n=6, $p<0.05$) at HPs of −80 and −40 mV, respectively (Fig. 1d). The stimulatory effect of Bay K-8644 on $I_{Ca,SS}$ was blocked by nifedipine by 81.1±7.2% and 72.3±6.5% at −80 and −40 mV HPs, respectively (Fig. 1d). However, both Bay K-8644 and nifedipine failed to affect the $I_{Ca,peak}$ (Fig. 1d). Thus, $I_{Ca,SS}$ was referred to as L-type VDCCs in this study.

Inhibition of L-type VDCCs by exogenous H_2S in pancreatic islet beta cells With the HP at −80 mV, NaHS significantly inhibited the $I_{Ca,SS}$ by 31.3±2.4% (n=12, $p<0.05$), but not the $I_{Ca,peak}$ (at +10 mV, n=12, $p>0.05$) (Figs 2a,c and 3a). The inhibitory effect of NaHS on L-type VDCCs was reversible

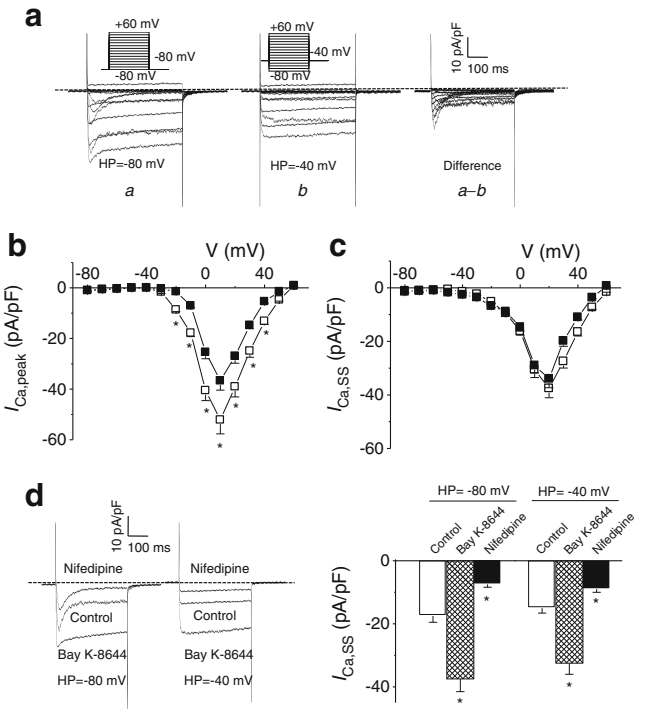

Fig. 1 VDCC currents in mouse pancreatic beta cells. (**a**) Original VDCC traces recorded from −80 mV to +60 mV with HPs of −80 mV (*a*) and −40 mV (*b*), respectively, and the differential currents (*a*−*b*) generated after subtracting the current recorded in (*b*) from those in (*a*). (**b**) The *I*–*V* relationship of $I_{Ca,peak}$ recorded with different HPs (−80 and −40 mV) is summarised (n=8, p<0.05). The $I_{Ca,peak}$ is measured at the maximum amplitude of I_{Ca} at each testing potential. (**c**) The *I*–*V* relationship of $I_{Ca,SS}$ recorded with different HPs of −40 mV (black squares) and −80 mV (white squares) is summarised (n=8). The $I_{Ca,SS}$ is measured at the end of each testing pulse. (**d**) Original VDCC traces recorded at the testing potential of +10 mV with different HPs in the absence and presence of 0.2 μmol/l Bay K-8644 and 1 μmol/l nifedipine. The dotted line indicates zero current. The summary shows $I_{Ca,SS}$ before and after the application of Bay K-8644 and nifedipine (test potential, +10 mV, n=6, *p<0.05)

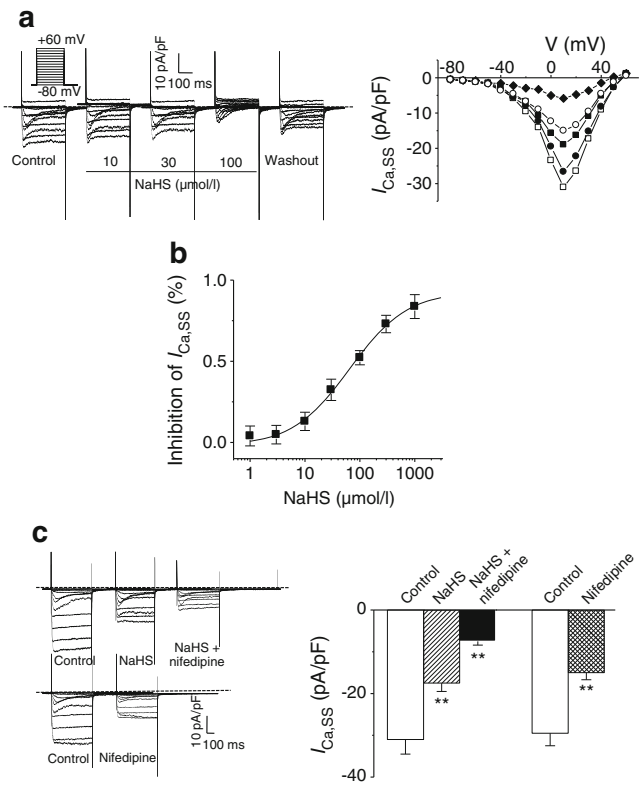

Fig. 2 The inhibitory effects of NaHS on VDCC currents in mouse pancreatic beta cells. (**a**) Original VDCC traces sequentially recorded in the same cell from –80 mV to +60 mV with an HP of –80 mV in the absence (white squares) and presence of different concentrations of NaHS (at 10 [black circles], 30 [black squares], and 100 [black diamonds] μmol/l) and chemical washout (white circles). The corresponding *I*–*V* relationship of $I_{Ca,SS}$ is shown in the right panel. (**b**) The concentration-dependent inhibition of $I_{Ca,SS}$ by NaHS (at +10 mV, HP=–80 mV, n=12) with IC_{50} of 65.4±5.6 μmol/l. (**c**) Original VDCC traces in the left panel showing that $I_{Ca,SS}$ was inhibited by NaHS (100 μmol/l), NaHS and nifedipine (1 μmol/l) as well as by nifedipine alone (TP=−80 to +60 mV, HP=−80 mV). The summary of these data is shown in the right panel, with current intensity measured at +10 mV (HP=−80 mV, n=5, **p<0.01)

after washing out NaHS (Fig. 2a). NaHS did not alter the reversal potential and the voltage-dependence of L-type VDCCs (Fig. 2a). The IC_{50} of the inhibitory effect of NaHS on L-type VDCCs was 65.4±5.6 μmol/l (Fig. 2b). The $I_{Ca,SS}$ was inhibited by NaHS by 43.5±4.4% and further inhibited by nifedipine by 32.3±3.5% (n=5, p<0.01) (Fig. 2c). After changing the HP to −40 mV from −80 mV, only the $I_{Ca,SS}$ existed and NaHS significantly inhibited $I_{Ca,SS}$ by 45.6±4.4% (Fig. 3b,c), confirming that NaHS targeted only L-type VDCCs. In general, NaHS did not shift the current–voltage (*I*–*V*) curve of L-type VDCCs with the HP at −80 mV (Figs 2 and 3). It appears that with a HP at −40 mV NaHS caused a marginal, but inapparent, shift of the *I*–*V* curve of L-type VDCCs to the left (Fig. 3b).

To evaluate the recovery from inactivation, currents were elicited by the double-pulse protocol, with the interval separating two pulses increased progressively from 0 to 200 ms (Fig. 3d). When the interval was short, the I_{Ca} was small and decayed more slowly. An increase in the interval between the conditioning pulse and test pulse resulted in a recovery of I_{Ca}. The time constants (τ) of I_{Ca} recovery from inactivation in the HP of −70 mV were 89.4±6.3 and 115.4±8.5 ms in the control and NaHS group, respectively (Fig. 3d). As the time interval (*t*) increased to 80–200 ms, the I/I_{max} values in the NaHS-treated group were significantly decreased in comparison with those of the control group (n=6, p<0.05) (Fig. 3d). It appears that L-type VDCCs in INS-1E cells take more than 70 ms for recovery from inactivation. The mechanism underlying this delayed recovery is not clear yet.

ACS 67 is an analogue of latanoprost (an F-series prostaglandin analogue) that contains an H_2S-releasing component conjugated to the latanoprost carboxyl group, and is therefore a lipid-soluble, slow-releasing H_2S donor [20].

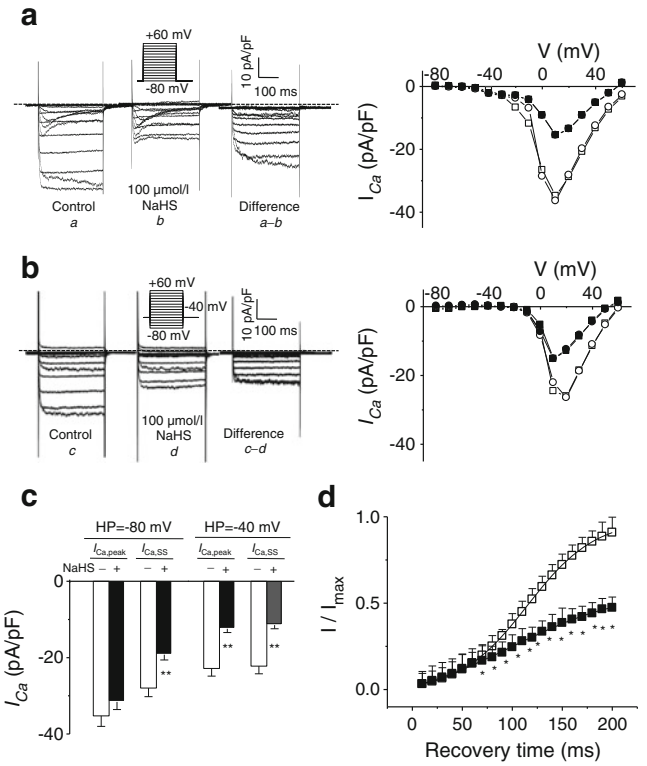

Fig. 3 The inhibition of VDCC currents by NaHS at different HPs in mouse pancreatic beta cells. (**a**) Original VDCC traces recorded from −80 to +60 mV with an HP of −80 mV before (*a*) and after (*b*) the application of NaHS (at 100 μmol/l). The corresponding *I–V* relationship of $I_{Ca,\ peak}$ before (white squares) and after (black squares) the application of 100 μmol/l NaHS, and that of $I_{Ca,SS}$ before (white circles) and after (black circles) NaHS application. (**b**) Original VDCC traces recorded with an HP of −40 mV before (*c*) and after (*d*) NaHS application. The corresponding *I–V* relationships of $I_{Ca,\ peak}$ and $I_{Ca,SS}$ are shown in the right panel. (**c**) Summary of the inhibitory effect of NaHS on the peak and steady-state I_{Ca} currents at +10 mV at different HPs (−80 and −40 mV) (n=10, $^{**}p<0.01$). (**d**) The effect of NaHS on the recovery kinetics from VDCC inactivation. A double-pulse protocol is shown with the testing potentials stepped from −70 to 0 mV at an HP of −80 mV. The interval between two pulses ranges from 0 ms to 200 ms at 10 ms increments. A downward shift of the recovery curve was observed in the presence of NaHS (black squares) in comparison with the curve in the absence of NaHS (white squares) (n=6, $^{*}p<0.05$)

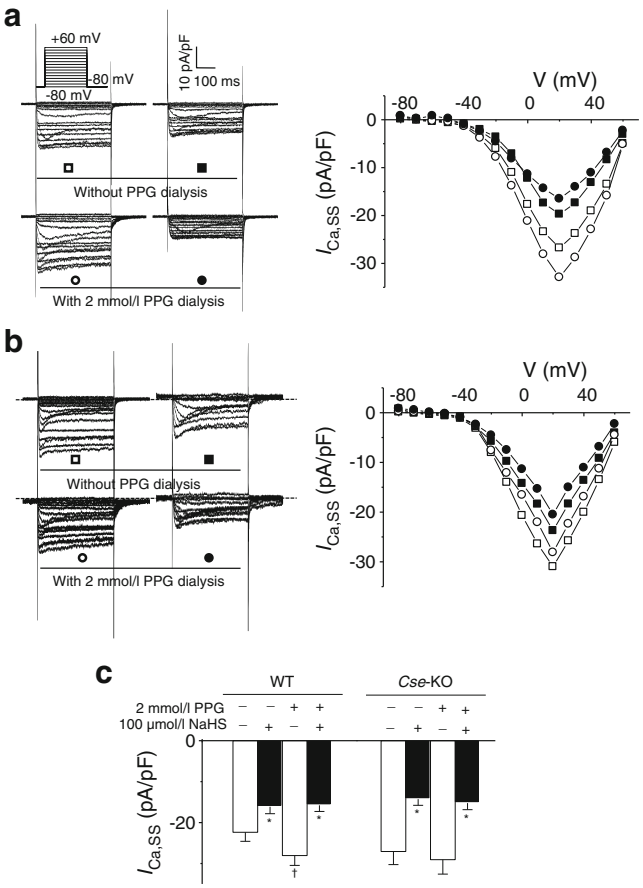

Fig. 4 The effect of NaHS on VDCC currents in the absence and presence of PPG dialysis of pancreatic beta cells from WT and *Cse*-KO mice. (**a**) The representative VDCC traces for inward $I_{Ca,SS}$ currents recorded in WT mouse pancreatic beta cells with an HP at −80 mV before and after the application of NaHS in the absence and presence of PPG dialysis. The corresponding *I–V* relationship curves of $I_{Ca,SS}$ are shown in the right panel, either without PPG in the absence (white squares) and presence (black squares) of 100 μmol/l NaHS or with 2 mmol/l PPG dialysis in the absence (white circles) and presence (black circles) of NaHS. (**b**) The representative $I_{Ca,SS}$ current traces in *Cse*-KO mouse pancreatic beta cells with the same recording conditions as in (a). The corresponding *I–V* relationship curves of $I_{Ca,SS}$ are shown in the right panel. (**c**) Summary of the effects of NaHS on $I_{Ca,SS}$, measured at +10 mV without or with 2 mmol/l PPG dialysis of WT and *Cse*-KO pancreatic beta cells (HP=−80 mV, n=10, $^{*}p<0.05$ for 100 μmol/l NaHS vs control, $^{\dagger}p<0.05$ for 2 vs 0 mmol/l PPG dialysis)

ACS 67 (100 μmol/l) also inhibits L-type Ca^{2+} channels. It decreased L-type VDCC currents by 18.3±2.8% at a membrane potential of +10 mV (n=5, $p<0.05$). However, the inhibitory effect of ACS 67 was weaker than that of NaHS at the same concentration (45.4±4.6% inhibition).

Effects of endogenous H_2S on L-type VDCCs in pancreatic islet beta cells Without PPG dialysis, NaHS at 100 μmol/l significantly inhibited $I_{Ca,SS}$ by 27.5±3.2% (at +20 mV, n=10, $p<0.05$) in WT beta cells (Fig. 4a,c). By including 2 mmol/l PPG in the pipette solution, NaHS also inhibited $I_{Ca,SS}$ by 43.8±5.6% (at +20 mV, n=10) (Fig. 4a,c). On the other hand, NaHS inhibited $I_{Ca,SS}$ in *Cse*-KO mouse beta cells with and without PPG dialysis by 25.2±3.0% and 32.2±4.3%, respectively (at +20 mV, n=10, $p<0.05$), but PPG dialysis did not alter basal $I_{Ca,SS}$ level in *Cse*-KO mouse beta cells (Fig. 4b,c). To test the effect of endogenous H_2S on $I_{Ca,SS}$, *Cse*-KO mice were used to isolate pancreatic beta cells. NaHS significantly suppressed $I_{Ca,SS}$ by 29.7±3.5% and 55.6±6.4% in WT and *Cse*-KO mouse beta cells, respectively (n=10, $p<0.01$) (Fig. 5a–c). The basal current density of $I_{Ca,SS}$ in beta cells from *Cse*-KO mice was greater than that from WT mice ($p<0.05$) (Fig. 5c).

Effects of the CSE/H_2S system on insulin release from pancreatic islets Following incubation with culture medium and normal

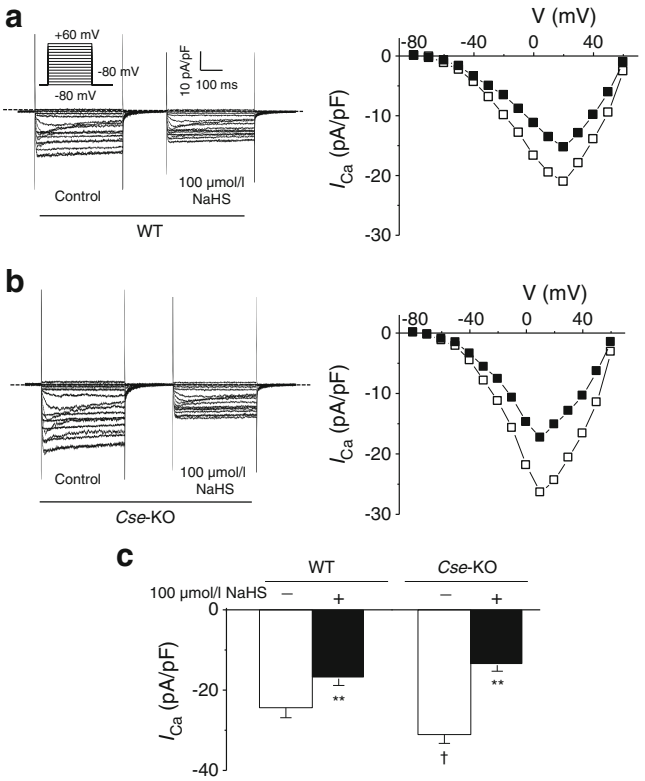

Fig. 5 The effect of NaHS on VDCC currents in pancreatic beta cells from *Cse*-KO mice. (**a**) The representative inward $I_{Ca,SS}$ current traces in WT mouse pancreatic beta cells (HP=–80 mV) before and after the application of NaHS. The corresponding *I–V* relationship curves before (white squares) and after (black squares) the application of 100 μmol/l NaHS are shown in the right panel. (**b**) The representative $I_{Ca,SS}$ current traces in *Cse*-KO mouse pancreatic beta cells with the same recording condition as in (a). The corresponding *I–V* relationship curves are shown in the right panel. (**c**) Summary of the effects of NaHS on $I_{Ca,SS}$ currents, measured at +10 mV, in pancreatic beta cells from WT and *Cse*-KO mice (HP=–80 mV, n=10; **p<0.01 for 100 μmol/l NaHS vs control; $^{\dagger}p$<0.05 for *Cse*-KO vs WT)

glucose (at 10 mmol/l) for 30 min, insulin release from freshly isolated islets from *Cse*-KO mice was much higher than that from WT islets (n=5, p<0.05) (Fig. 6a). Insulin secretion from islets was inhibited by nifedipine by 45.7±3.6% and 41.2±4.5% in WT and *Cse*-KO islets, respectively. NaHS at 100 μmol/l and 300 μmol/l inhibited glucose-stimulated insulin secretion by 26.7±4.5% and 49.5±6.5% (n=5, p<0.05 vs control), respectively (Fig. 6b). NaHS or nifedipine alone inhibited insulin release, and their co-application had an increased effect (n=5, p>0.05) (Fig. 6c). Bay K-8644 alone enhanced insulin secretion in mouse islets, but co-application of NaHS or nifedipine counteracted the stimulatory effect of Bay K-8644 (Fig. 6c). These results suggest that nifedipine and H_2S may inhibit the same L-type VDCCs. Glibenclamide alone increased insulin secretion, which was also inhibited by the addition of NaHS (n=5, p<0.05) (Fig. 6c). This result indicates that K_{ATP} channel activation is involved in the regulation of insulin release. Figure 6d further shows the inhibitory effect of endogenous H_2S on insulin release from islets of WT or *Cse*-KO mice, assayed in KRB.

Discussion

We and others have previously shown that H_2S functions as an endogenous opener of K_{ATP} channels in different types of cell, including smooth muscle cells [2, 21], HEK-293 cells [22] and pancreatic beta cells [5, 11], independent of the activation of cytosolic second messengers. Interaction between H_2S and K_{ATP} channels in insulin-secreting cells may underlie an important mechanism for the regulation of insulin secretion from pancreatic beta cells. Our present study examined the effects of exogenous and endogenous H_2S on L-type VDCCs in mouse pancreatic beta cells. We have found that: (1) the H_2S donors NaHS and ACS 67 reversibly inhibited L-type VDCCs; (2) PPG dialysis to inhibit CSE activity and lower endogenous H_2S level increased the basal amplitude of L-type VDCCs in WT mouse beta cells; and (3) the density of L-type VDCCs in beta cells from *Cse*-KO mice, in which the endogenous H_2S level is minimised, is greater than that from WT mice. These data represent the first evidence that H_2S has an inhibitory role in the regulation of L-type VDCCs in mouse pancreatic beta cells.

Glucose stimulation of pancreatic beta cells involves membrane depolarisation and Ca^{2+} influx. An upsurge in $[Ca^{2+}]_i$ triggers the exocytotic machinery, with subsequent insulin release. Ca^{2+} influx in beta cells occurs primarily through VDCCs, especially L-type VDCCs [23–25]. L-type VDCCs, a large hetero-oligomeric complex consisting of α_1-, α_2/δ-, β- and γ-subunits, is characterised by high-voltage-activated persistent Ca^{2+} currents that are without inactivation or inactivate slowly. L-type VDCCs are blocked by nifedipine or verapamil and activated by Bay K-8644 or CGP28391 [26]. N- and R-type VDCCs have been reported in mouse beta cells [27]. These VDCCs belong to the same group of high-voltage-activated VDCCs as L-type channels. However, N and R channels can be blocked by ω-conotoxin and SNX482, respectively, but L-channels are sensitive to dihydropyridines. In our study, the blockade of L-type VDCCs by nifedipine and its stimulation by Bay K-8644 indicate that the L-type VDCCs currents recorded are unlikely to have been contaminated by N- or R-type VDCCs. On the other hand, the effects of H_2S on N- and R-type VDCCs in beta cells cannot yet be excluded.

T-type VDCCs have been suggested to involve modulation of general membrane electrical activity to enhance insulin secretion [28]. They are activated at more negative membrane potentials and are inactivated quickly and completely [29]. T-type VDCCs have been recorded in mouse

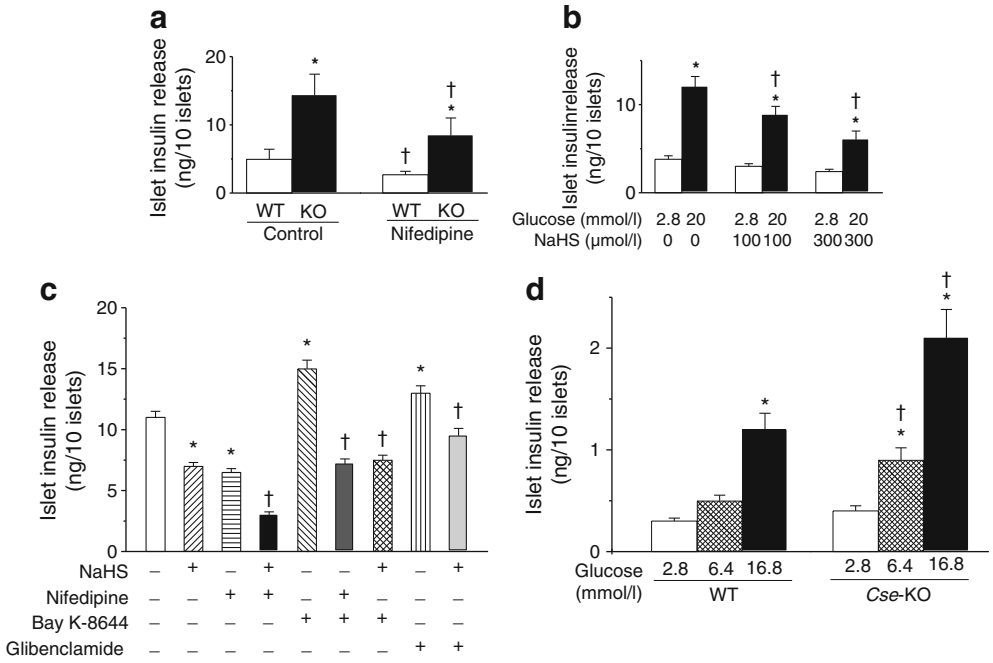

Fig. 6 Insulin secretion and H_2S production of pancreatic islets from WT and *Cse*-KO mice. (**a**) Glucose (10 mmol/l)-stimulated insulin secretion from WT and *Cse*-KO mouse islets and its inhibition by nifedipine (1 μmol/l) (n=5, *p<0.05 for KO vs WT; †p<0.05 nifedipine vs control). (**b**) The effects of NaHS on insulin secretion from WT mouse islets (n=5, *p<0.05 for 20 mmol/l vs 2.8 mmol/l glucose; †p<0.05 for 100/300 vs 0 μmol/l NaHS). (**c**) Effects of NaHS (100 μmol/l), nifedipine (1 μmol/l), Bay K-8644 (0.2 μmol/l), and glibenclamide (30 μmol/l) on 20 mmol/l glucose-stimulated insulin secretion from WT mouse islets (n=5, *p<0.05 for different treatments with NaHS, nifedipine, Bay K-8644, and glibenclamide vs control without treatment; †p<0.05 for NaHS+Bay K-8644 vs Bay K-8644, and NaHS+glibenclamide vs glibenclamide). Mouse islets were incubated with RPMI-1640 medium in experiments shown in (a–c). (**d**) Insulin secretion from mouse islets incubated in KRB; n=4; *p<0.05 for 16.8 mmol/l or 6.4 mmol/l vs 2.8 mmol/l; †p<0.05 for KO vs WT at 6.4 or 16.8 mmol/l glucose

beta cells by others [18, 30, 31] and are likely to have been recorded in our present study. As we focused on the effects of H_2S on L-type VDCCs, no further effort was taken to characterise T-type VDCCs in our study.

Both CSE and cystathionine β-synthase (CBS) are produced in rodent pancreatic tissues or cloned islet beta cell lines, while CSE plays a more important role in endogenous H_2S production in beta cells. The expression level of *Cse* mRNA was significantly higher than that of CBS in pancreatic islets and PPG abolished most of the H_2S production in pancreatic islets and INS-1E cells [5, 6]. Furthermore, H_2S production in pancreatic beta cells is decreased by increased blood glucose level [7]. Overexpression of *Cse* inhibited insulin release from INS-1E cells, and lowering endogenous H_2S production by PPG or *Cse*-targeted small interfering RNA had the opposite effect [5]. We previously showed that PPG ameliorated high blood glucose of ZDF rats to near normal levels, while amino-oxyacetate, a specific blocker of CBS, did not significantly change the hyperglycaemic status of ZDF rats [6]. Furthermore, H_2S production rate was significantly decreased in pancreatic islets from *Cse*-KO mice and PPG treatment drastically reduced H_2S production rate in pancreatic islets from WT mice [4]. In addition, L-cysteine and H_2S inhibit glucose-stimulated insulin secretion from insulin-secreting beta cell lines (INS-1E, MIN6 and HIT-T15) and isolated rat islets [5, 11]. All these data suggest a critical role of CSE in producing H_2S in beta cells, thus regulating insulin secretion under physiological or pathological conditions.

L-type VDCC play a crucial role in the regulation of insulin secretion in pancreatic beta cells. The decay of $I_{Ca,SS}$ during depolarisation is called inactivation, and is regulated by elevation of $[Ca^{2+}]_i$ as well as by membrane depolarisation [32, 33]. Therefore, $[Ca^{2+}]_i$ in the vicinity of the channels critically controls their activity during stimulus–secretion coupling. The Ca^{2+}-dependent process of inactivation may serve as a negative feedback mechanism for regulating Ca^{2+} entry into pancreatic beta cells and insulin granule exocytosis [32]. The recovery from inactivation of $I_{Ca,SS}$ is affected by different factors, such as the HP, the voltage and duration of the conditioning pulse, the frequency of the coupled pulses and the extracellular ionic milieu. H_2S inhibits $I_{Ca,SS}$ and delays the channels' recovery from inactivation in beta cells, producing a negative feedback regulation on $[Ca^{2+}]_i$.

Glucose-stimulated insulin secretion was examined in our study with different manipulations of H_2S level and function status of L-type VDCCs. NaHS at different concentrations had no statistically significant effect on basal insulin secretion with 2.8 mmol/l glucose (Fig. 6b). On the other hand, a significant portion of insulin release from pancreatic islets of *Cse*-KO mice remained in the presence of nifedipine (Fig. 6a). This result is not in conflict with the notion that H_2S inhibits L-type VDCCs to decrease insulin release. H_2S has multiple effects on insulin metabolism in the pancreas. We have previously demonstrated that H_2S induces pancreatic beta cell apoptosis and decreases beta cell mass, thus reducing insulin production [4]. The diminished endogenous H_2S in *Cse*-KO islets would increase pancreatic beta cell mass and more insulin would be produced, so that with the same concentration of nifedipine treatment more insulin would be available for release. Glibenclamide alone increased glucose-stimulated insulin release, which was partially suppressed by NaHS. This suggests that H_2S-inhibited insulin release relies on K_{ATP}-channel-dependent and -independent mechanisms. The former is mediated by the indirect inactivation of L-type VDCCs by H_2S via activation of K_{ATP} channels and membrane hyperpolarisation, whereas the latter involves direct inhibition of L-type VDCCs by H_2S. No matter whether K_{ATP} channels or L-type VDCCs or both are affected by H_2S, the inhibition of L-type VDCCs, leading to lowered $[Ca^{2+}]_i$, is the final coupling node between the cellular electrophysiological changes and the reduced insulin release induced by H_2S.

In summary, we report an original observation that H_2S, applied exogenously or generated endogenously, inhibits L-type VDCCs and regulates insulin secretion. This inhibitory effect of H_2S on L-type VDCC in pancreatic beta cells is independent of the effect of H_2S on K_{ATP} channels. As such, our report adds to current understanding of the regulation of pancreatic function by H_2S through its effects on different ion channels in beta cells. This will pave the way for targeting different ion channels when devising selective therapeutic strategies to correct abnormal H_2S metabolism in the pancreas under different pathological conditions.

Funding This work was supported by an operating grant from the Canadian Diabetes Association (to R. Wang) and a post-doctoral fellowship from the Heart and Stroke Foundation of Canada (to G. Tang).

Duality of interest The authors declare that there is no duality of interest associated with this manuscript.

Contribution statement All authors have: made substantial contributions to conception and design, acquisition of data, analysis and interpretation of data; drafted the article or revised it critically for important intellectual content; and given final approval of the version to be published.

References

1. Zhao W, Ndisang JF, Wang R (2003) Modulation of endogenous production of H_2S in rat tissues. Can J Physiol Pharmacol 81:848–853
2. Zhao W, Zhang J, Lu Y, Wang R (2001) The vasorelaxant effect of H_2S as a novel endogenous gaseous K_{ATP} channel opener. EMBO J 20:6008–6016
3. Yang G, Wu L, Jiang B et al (2008) H_2S as a physiologic vasorelaxant: hypertension in mice with deletion of cystathionine gamma-lyase. Science 322:587–590
4. Yang G, Tang G, Zhang L, Wu L, Wang R (2011) The pathogenic role of cystathionine gamma-lyase/hydrogen sulfide in streptozotocin-induced diabetes in mice. Am J Pathol 79:869–879
5. Yang W, Yang G, Jia X, Wu L, Wang R (2005) Activation of K_{ATP} channels by H_2S in rat insulin-secreting cells and the underlying mechanisms. J Physiol 569:519–531
6. Wu L, Yang W, Jia X, Yang G, Duridanova D, Cao K, Wang R (2009) Pancreatic islet overproduction of H_2S and suppressed insulin release in Zucker diabetic rats. Lab Invest 89:59–67
7. Zhang L, Yang G, Tang G, Wu L, Wang R (2011) Rat pancreatic level of cystathionine γ-lyase is regulated by glucose level via specificity protein 1 (SP1) phosphorylation. Diabetologia 54:2615–2625
8. Yusuf M, Kwong Huat BT, Hsu A, Whiteman M, Bhatia M, Moore PK (2005) Streptozotocin-induced diabetes in the rat is associated with enhanced tissue hydrogen sulfide biosynthesis. Biochem Biophys Res Commun 333:1146–1152
9. Tang G, Wu L, Wang R (2010) Interaction of hydrogen sulfide with different ion channels. Clin Exp Pharmacol Physiol 37:753–763
10. Ashcroft FM, Rorsman P (1989) Electrophysiology of the pancreatic beta-cell. Prog Biophys Mol Biol 54:87–143
11. Ali MY, Whiteman M, Low CM, Moore PK (2007) Hydrogen sulphide reduces insulin secretion from HIT-T15 cells by a K_{ATP} channel-dependent pathway. J Endocrinol 195:105–112
12. Sun YG, Cao YX, Wang WW, Ma SF, Yao T, Zhu YC (2008) Hydrogen sulphide is an inhibitor of L-type calcium channels and mechanical contraction in rat cardiomyocytes. Cardiovasc Res 79:632–641
13. García-Bereguiaín MA, Samhan-Arias AK, Martín-Romero FJ, Gutiérrez-Merino C (2008) Hydrogen sulfide raises cytosolic calcium in neurons through activation of L-type Ca^{2+} channels. Antioxid Redox Signal 10:31–42
14. Wang R, Karpinski E, Pang PKT (1989) Two types of voltage-dependent calcium channels in isolated smooth muscle cells from rat tail artery. Am J Physiol Heart Circ Physiol 256:H1361–H1368
15. Wang R, Wu Y, Tang G, Wu L, Hanna ST (2000) Altered L-type Ca^{2+} channel currents in vascular smooth muscle cells from experimental diabetic rats. Am J Physiol Heart Circ Physiol 278:H714–H722
16. Göpel SO, Kanno T, Barg S, Weng XG, Gromada J, Rorsman P (2000) Regulation of glucagon release in mouse-cells by K_{ATP} channels and inactivation of TTX-sensitive Na^+ channels. J Physiol 528:509–520
17. Mears D, Zimliki CL (2004) Muscarinic agonists activate Ca^{2+} store-operated and -independent ionic currents in insulin-secreting HIT-T15 cells and mouse pancreatic beta-cells. J Membr Biol 197:59–70

18. Hopkins WF, Satin LS, Cook DL (1991) Inactivation kinetics and pharmacology distinguish two calcium currents in mouse pancreatic B cells. J Membr Biol 119:229–239
19. Plant TD (1988) Properties and calcium-dependent inactivation of calcium currents in cultured mouse pancreatic B cells. J Physiol 404:731–747
20. Perrino E, Uliva C, Lanzi C, Soldato PD, Masini E, Sparatore A (2009) New prostaglandin derivative for glaucoma treatment. Bioorg Med Chem Lett 19:1639–1642
21. Tang G, Wu L, Liang W, Wang R (2005) Direct stimulation of K_{ATP} channels by exogenous and endogenous hydrogen sulfide in vascular smooth muscle cells. Mol Pharmacol 68:1757–1764
22. Jiang B, Tang G, Cao K, Wu L, Wang R (2010) Molecular mechanism for H_2S-induced activation of K_{ATP} channels. Antioxid Redox Signal 12:1167–1178
23. Keahey HH, Rajan AS, Boyd AE 3rd, Kunze DL (1989) Characterization of voltage-dependent Ca^{2+} channels in beta-cell line. Diabetes 38:188–193
24. Namkung Y, Skrypnyk N, Jeong MJ et al (2001) Requirement for the L-type Ca^{2+} channel alpha-1D subunit in postnatal pancreatic beta cell generation. J Clin Invest 108:1015–1022
25. Schulla V, Renström E, Feil R et al (2003) Impaired insulin secretion and glucose tolerance in beta cell-selective $Ca_v1.2$ Ca^{2+} channel null mice. EMBO J 22:3844–3854
26. Catterall WA (1991) Functional subunit structure of voltage-gated calcium channels. Science 253:1499–1500
27. Jing X, Li DQ, Olofsson CS et al (2005) CaV2.3 calcium channels control second-phase insulin release. J Clin Invest 115:146–154
28. Bhattacharjee A, Whitehurst RM Jr, Zhang M (1997) T-type calcium channels facilitate insulin secretion by enhancing general excitability in the insulin-secreting cell line, INS-1E. Endocrinology 138:3735–3740
29. Hiriart M, Matteson DR (1988) Na channels and two types of Ca^{2+} channels in rat pancreatic B cells identified with the reverse hemolytic plaque assay. J Gen Physiol 91:617–639
30. Wang L, Bhattacharjee A, Fu J, Li M (1996) Abnormally expressed low voltage-activated calcium channels in beta-cells from NOD mice and a related clonal cell line. Diabetes 45:1678–1683
31. Wang L, Bhattacharjee A, Zuo Z et al (1999) A low voltage-activated Ca^{2+} current mediates cytokine-induced pancreatic β-cell death. Endocrinology 140:1200–1204
32. Lee KS, Marban E, Tsien RW (1985) Inactivation of calcium channels in mammalian heart cells: joint dependence on membrane potential and intracellular calcium. J Physiol 364:395–411
33. Imredy JP, Yue DT (1994) Mechanism of Ca^{2+}-sensitive inactivation of L-type Ca^{2+} channels. Neuron 12:1301–1318